

UCD-03-4
 IFIC/03-19
 LPT 03-35
 SHEP-03-08
 hep-ph/0305109
 April, 2003

Towards a No-Lose Theorem for NMSSM Higgs Discovery at the LHC

ULRICH ELLWANGER¹, JOHN F. GUNION², CYRIL HUGONIE³ AND STEFANO MORETTI⁴

¹*Laboratoire de Physique Théorique,
 Université de Paris XI, Bâtiment 210, F-91405 ORSAY Cedex, France*

²*Davis Institute for High Energy Physics,
 University of California, Davis, California 95616, USA*

³*AHEP Group, Instituto de Física Corpuscular – CSIC/Universitat de València,
 Edificio Institutos de Investigación, Apartado de Correos 22085, E-46071 València, Spain*

⁴*Department of Physics and Astronomy, University of Southampton,
 Southampton, SO17 1BJ, UK*

Abstract

We scan the parameter space of the NMSSM for the observability of a Higgs boson at the LHC with 300 fb^{-1} integrated luminosity per detector, taking the present LEP constraints into account. We focus on the regions of parameter space for which none of the usually considered LHC detection modes are viable due to the fact that the only light non-singlet (and, therefore, potentially visible) Higgs boson, h , decays mainly to two CP-odd light Higgs bosons, $h \rightarrow aa$. We simulate the $WW \rightarrow h \rightarrow aa$ detection mode. We find that this signal may be detectable at the LHC as a signal/background $\sim (500-1000)/300$ bump in the tail of a rapidly falling mass distribution. If further study gives us confidence that the shape of the background tail is predictable, then we can conclude that NMSSM Higgs detection at the LHC will be possible throughout all of parameter space by combining this signal with the usual detection modes previously simulated by ATLAS and CMS. We also show that this $WW \rightarrow h \rightarrow aa$ signal will be highly visible at the LC due to its cleaner environment and high luminosity. We present a study of the production modes and decay channels of interest at the LC.

1 Introduction

One of the most attractive supersymmetric models is the Next to Minimal Supersymmetric Standard Model (NMSSM) [1, 2, 3, 4], which extends the MSSM by the introduction of just one single superfield, \widehat{S} . When the scalar component of \widehat{S} acquires a TeV scale vacuum expectation value (a very natural result in the context of the model), the superpotential term $\widehat{S}\widehat{H}_u\widehat{H}_d$ generates an effective $\mu\widehat{H}_u\widehat{H}_d$ interaction for the Higgs doublet superfields. Such a term is essential for acceptable phenomenology. No other SUSY model generates this crucial component of the superpotential in as natural a fashion. Thus, the phenomenological implications of the NMSSM at future accelerators should be considered very seriously. One aspect of this is the fact that the h, H, A, H^\pm Higgs sector of the MSSM is extended so that there are three CP-even Higgs bosons ($h_{1,2,3}, m_{h_1} < m_{h_2} < m_{h_3}$), two CP-odd Higgs bosons ($a_{1,2}, m_{a_1} < m_{a_2}$) (we assume that CP is not violated in the Higgs sector) and a charged Higgs pair (h^\pm). An important question is then the extent to which the no-lose theorem for MSSM Higgs boson discovery at the LHC (after LEP constraints) is retained when going to the NMSSM; *i.e.* is the LHC guaranteed to find at least one of the $h_{1,2,3}, a_{1,2}, h^\pm$?

One of the key ingredients in the no-lose theorem for MSSM Higgs boson discovery is the fact that decays of the SM-like Higgs boson to AA are only possible if m_A is quite small. This is due to the fact that the masses of the h, H, A, H^\pm of the MSSM are closely tied to one another. In particular, m_A can only be small if m_h is also relatively small and $m_{H^\pm} \sim m_W$. In this region, it is the H that is SM-like. The small- m_A region is either excluded by LEP because of non-observation of hA production, or will be detectable at the LHC via observation of $t \rightarrow bH^\pm$ decays in $t\bar{t}$ production. Most of the still unconstrained portion of MSSM parameter space corresponds to the decoupling region of $m_A \sim m_H \sim m_{H^\pm} > 120 - 130$ GeV in which the h is SM-like and $m_h \lesssim 120 - 130$ GeV so that $h \rightarrow AA$ decays are forbidden. In the NMSSM, these strong mass relations are weakened. The h_1 or h_2 can be SM-like without the a_1 necessarily being heavy. As a result, $h_1 \rightarrow a_1 a_1$ or $h_2 \rightarrow a_1 a_1$ decays can be prominent and fall outside the scope of the usual detection modes for the SM-like MSSM h on which the MSSM no-lose LHC theorem largely relies.

In Ref. [5], a partial no-lose theorem for NMSSM Higgs boson discovery at the LHC was established. In particular, it was shown that the LHC would be able to detect at least one of the NMSSM Higgs bosons (typically, one of the lighter CP-even Higgs states) throughout the full parameter space of the model, excluding only those parameter choices for which there is sensitivity to the model-dependent decays of Higgs bosons to other Higgs bosons and/or superparticles. Here, we will retain the assumption of a heavy superparticle spectrum and address the question of whether or not this no-lose theorem can be extended to those regions of NMSSM parameter space for which Higgs bosons can decay to other Higgs bosons. We find that the parameter choices such that the “standard” discovery modes fail *would* allow Higgs boson discovery if detection of $h \rightarrow aa$ decays is possible. (When used generically, the symbol h will now refer to $h = h_1, h_2$ or h_3 and the symbol a will refer to $a = a_1$ or a_2). Detection of $h \rightarrow aa$ will be difficult since each a will decay primarily to either $b\bar{b}$ (or 2 jets if $m_a < 2m_b$) and $\tau^+\tau^-$, yielding final states that will typically have large backgrounds at the LHC. Further, a light a can only be detected on its own at the LHC if it has a highly enhanced Yukawa coupling to b (or t) quarks.

Let us begin by reviewing our earlier procedure. For each point in parameter space not ruled out by constraints from LEP on Higgs boson production, $e^+e^- \rightarrow Zh$ [6] or

associated production $e^+e^- \rightarrow ha$ [7], we calculate the Higgs boson masses and decay branching ratios including all the relevant radiative corrections. We eliminate parameter choices for which one Higgs boson can decay to two other Higgs bosons or a vector boson plus a Higgs boson. For the remaining regions of parameter space, we then estimate the statistical significances (computed as $N_{SD} = S/\sqrt{B}$ for a given mode) for all Higgs boson detection modes so far studied at the LHC [8, 9, 10, 11]. These are (with $\ell = e, \mu$)

- 1) $gg \rightarrow h/a \rightarrow \gamma\gamma$;
- 2) associated Wh/a or $t\bar{t}h/a$ production with $\gamma\gamma\ell^\pm$ in the final state;
- 3) associated $t\bar{t}h/a$ production with $h/a \rightarrow b\bar{b}$;
- 4) associated $b\bar{b}h/a$ production with $h/a \rightarrow \tau^+\tau^-$;
- 5) $gg \rightarrow h \rightarrow ZZ^{(*)} \rightarrow 4 \text{ leptons}$;
- 6) $gg \rightarrow h \rightarrow WW^{(*)} \rightarrow \ell^+\ell^-\nu\bar{\nu}$;
- 7) $WW \rightarrow h \rightarrow \tau^+\tau^-$;
- 8) $WW \rightarrow h \rightarrow WW^{(*)}$.

The outcome is that, for an integrated luminosity of 300 fb^{-1} at the LHC, there are still regions in the parameter space with $< 5\sigma$ expected statistical significance for all Higgs boson detection modes so far studied in detail by ATLAS and CMS, *i.e.* modes 1) – 6) but not the W -fusion modes 7), 8). On the other hand, the expected statistical significance for at least one of the non- W -fusion modes is always above 3.6σ at 300 fb^{-1} , and the statistical significance obtained by combining (using the naive Gaussian procedure) all the non- W -fusion modes is at least 4.8σ . However, we found that all such cases are quite observable (at $\geq 10.1\sigma$) in one of the W -fusion modes (using theoretically estimated statistical significances for these modes). For all points in the scanned parameter space, statistical significances obtained by combining all modes, including W -fusion modes, are always $\gtrsim 10.7\sigma$. Thus, NMSSM Higgs boson discovery by just one detector with $L = 300 \text{ fb}^{-1}$ is essentially guaranteed for those portions of parameter space for which Higgs boson decays to other Higgs bosons or supersymmetric particles are kinematically forbidden.

In this work, we investigate the complementary part of the parameter space, where *at least one* Higgs boson decays to other Higgs bosons. To be more precise, we require at least one of the following decay modes to be kinematically allowed:

$$\begin{aligned} i) \quad & h \rightarrow h'h' , \quad ii) \quad h \rightarrow aa , \quad iii) \quad h \rightarrow h^\pm h^\mp , \quad iv) \quad h \rightarrow aZ , \\ v) \quad & h \rightarrow h^\pm W^\mp , \quad vi) \quad a' \rightarrow ha , \quad vii) \quad a \rightarrow hZ , \quad viii) \quad a \rightarrow h^\pm W^\mp . \end{aligned} \quad (1)$$

The observability at the LHC of Higgs bosons that decay in these ways has not been studied, except for some particular MSSM cases that are not applicable for the masses and Yukawa coupling strengths that are most relevant in the NMSSM context. After searching those regions of parameter space for which one or more of the decays *i*) – *viii*) is allowed, we found that the only subregions that would not be excluded by modes 1) – 8) correspond to NMSSM parameter choices for which (a) there is a light CP-even Higgs boson with substantial doublet content that decays mainly to two still lighter CP-odd Higgs states, $h \rightarrow aa$, and (b) all the other Higgs states are either dominantly singlet-like, implying highly suppressed production rates, or relatively heavy, decaying to $t\bar{t}$ or to one of the “difficult” modes *i*) – *viii*). In such cases, it seems evident that the best opportunity for detecting at least one of the NMSSM Higgs bosons is to employ $WW \rightarrow h$ production and develop techniques for extracting a visible signal for the $h \rightarrow aa$ final state. We have performed a detailed simulation of this signal and find that its detection may be possible

after accumulating 300 fb^{-1} in both the ATLAS and CMS detectors. The nominal statistical significance achieved is $> 30\sigma$ with $S/B > 1$. However, the signal only emerges on the tail of a rapidly falling background. A thorough understanding of and confidence in the shape of this background tail would be needed to claim detection of the $h \rightarrow aa$ signal. If further study and, ultimately, actual measurements of the background outside the signal region result in such confidence then the combined search for this signal and the signals for Higgs bosons in the previously studied modes 1) – 8) would result in detection of at least one of the NMSSM Higgs bosons throughout the entire NMSSM parameter space (assuming no large branching ratios for Higgs boson decays to sparticles). Having reached this conclusion, we turn to a study of the role that a future LC will play in exploring the NMSSM Higgs sector for those parameter choices for which detecting the $h \rightarrow aa$ signal is so critical. We find, regardless of what happens at the LHC, that the LC is guaranteed to find one or more Higgs bosons, including detection of the $h \rightarrow aa$ signal in several different production channels, leading to the possibility of measuring the $h \rightarrow aa$ branching ratio.

In section 2, we review the basic set up of the NMSSM as well as our scanning procedure for the NMSSM parameter space. In section 3, we give a selection of benchmark points for which all statistical significances at the LHC are below 5σ after employing the standard discovery modes 1) – 8). We then discuss possible new discovery channels in section 4 together with our simulation results both at the LHC and the LC. Conclusions are given in section 5.

2 NMSSM Parameters

We consider the simplest version of the NMSSM [1, 3, 4], where the term $\mu \hat{H}_1 \hat{H}_2$ in the superpotential of the MSSM is replaced by (we use the notation \hat{A} for the superfield and A for its scalar component field)

$$\lambda \hat{H}_1 \hat{H}_2 \hat{S} + \frac{\kappa}{3} \hat{S}^3 , \quad (2)$$

so that the superpotential is scale invariant. We make no assumption on “universal” soft terms. Hence, the five soft supersymmetry breaking terms

$$m_{H_1}^2 H_1^2 + m_{H_2}^2 H_2^2 + m_S^2 S^2 + \lambda A_\lambda H_1 H_2 S + \frac{\kappa}{3} A_\kappa S^3 \quad (3)$$

are considered as independent. The masses and/or couplings of sparticles are assumed to be such that their contributions to the loop diagrams inducing Higgs boson production by gluon fusion and Higgs boson decay into $\gamma\gamma$ are negligible. In the stop sector, which appears in the radiative corrections to the Higgs potential, we chose the soft masses $m_Q = m_T \equiv M_{susy} = 1 \text{ TeV}$, and vary the stop mixing parameter

$$X_t \equiv 2 \frac{A_t^2}{M_{susy}^2 + m_t^2} \left(1 - \frac{A_t^2}{12(M_{susy}^2 + m_t^2)} \right) . \quad (4)$$

As in the MSSM, the value $X_t = \sqrt{6}$ – so called maximal mixing – maximizes the radiative corrections to the Higgs boson masses, and we found that it leads to the most challenging points in the parameter space of the NMSSM.

Assuming that the Higgs sector is CP conserving, the independent parameters of the model are thus: $\lambda, \kappa, m_{H_1}^2, m_{H_2}^2, m_S^2, A_\lambda$ and A_κ . For purposes of scanning and analysis, it is more convenient to eliminate $m_{H_1}^2, m_{H_2}^2$ and m_S^2 in favor of M_Z , $\tan \beta$ and $\mu_{\text{eff}} = \lambda \langle S \rangle$ through the three minimization equations of the Higgs potential (including the dominant 1- and 2-loop corrections [12]) and to scan over the six independent parameters

$$\lambda, \kappa, \tan \beta, \mu_{\text{eff}}, A_\lambda, A_\kappa. \quad (5)$$

We adopt the convention $\lambda, \kappa > 0$, in which $\tan \beta$ can have either sign. The absence of Landau singularities for λ and κ below the GUT scale ($\sim 2 \times 10^{16}$ GeV) imposes upper bounds on these couplings at the weak scale, which depend on the value of h_t and hence of $\tan \beta$ [1, 3]. Using $m_t^{\text{pole}} = 175$ GeV, one finds $\lambda_{\text{max}} \sim 0.69$ and $\kappa_{\text{max}} \sim 0.62$ for intermediate values of $\tan \beta$. In addition, we require $|\mu_{\text{eff}}| > 100$ GeV; otherwise a light chargino would have been detected at LEP. (The precise lower bound on $|\mu_{\text{eff}}|$ depends somewhat on $\tan \beta$ and the exact experimental lower bound on the chargino mass; however, our subsequent results do not depend on the precise choice of the lower bound on $|\mu_{\text{eff}}|$.)

We have performed a numerical scanning over the free parameters, which were randomly chosen in the following intervals:

$$0.1 < \lambda < \lambda_{\text{max}}, \quad 0.001 < \kappa < \kappa_{\text{max}}, \quad 2.5 < |\tan \beta| < 10, \\ 100 \text{ GeV} < |\mu_{\text{eff}}| < 500 \text{ GeV}, \quad 0 < |A_\lambda| < 500 \text{ GeV}, \quad 0 < |A_\kappa| < 500 \text{ GeV}. \quad (6)$$

For each point, we computed the CP-even and CP-odd Higgs boson masses and mixings, taking into account radiative corrections up to the dominant two loop terms, as described in [12]. The five mass eigenstates are denoted by h_i ($i = 1, 2, 3$) and a_j ($j = 1, 2$) for CP-even and CP-odd eigenstates respectively, with masses m_{h_i} and m_{a_j} in increasing order. We have eliminated parameter choices that lead to violation of the LEP constraints on Higgs boson production $e^+e^- \rightarrow Z h_i$ ($i = 1, 2$ or 3) [6]. These constraints give an upper bound on the $Z Z h_i$ reduced coupling, R_i , as a function of m_{h_i} . (The reduced coupling R_i is defined as the coupling $Z Z h_i$ divided by the corresponding Standard Model coupling and is the equivalent of $\sin(\beta - \alpha)$ in the MSSM.) We have also kept only parameters leading to consistency with the exclusion limit from LEP on Higgs bosons associated production $e^+e^- \rightarrow h_i a_j$ [7]. This provides an upper bound on the $Z h_i a_j$ reduced coupling, R'_{ij} , as a function of $m_{h_i} + m_{a_j}$ for $m_{h_i} \simeq m_{a_j}$ [7]. (The $Z h_i a_j$ reduced coupling is the equivalent of $\cos(\beta - \alpha)$ in the MSSM.) Finally, we calculated the charged Higgs boson mass m_{h^\pm} and required $m_{h^\pm} > 155$ GeV, so that $t \rightarrow h^\pm b$ would not be seen.

In order to probe the complementary part of the parameter space as compared to the scanning of Ref. [5], we required that at least one of the “difficult” decay modes $i) - viii)$ displayed in the previous section is allowed. For each Higgs state, we have calculated the branching ratios in the usual decay modes as well as in the difficult modes $i) - viii)$ when kinematically allowed. In doing so, we have included all relevant higher-order QCD corrections [13] using an adapted version of the FORTRAN code HDECAY [14]. We then estimated the expected statistical significances at the LHC in all Higgs boson detection modes $1) - 8)$ as described in the next section.

3 Invisible Points at the LHC

From the known couplings of the NMSSM Higgs scalars to gauge bosons and fermions it is straightforward to compute their production rates in gluon-gluon fusion and various associated production processes, as well as their partial widths into $\gamma\gamma$, gauge bosons and fermions, either relative to a SM Higgs scalar or relative to the MSSM h , H and/or A . This allows us to apply “NMSSM corrections” to the processes 1) – 8) of section 1. These NMSSM corrections are computed in terms of the following ratios: For the scalar Higgs bosons, R_i is the ratio of the coupling of the h_i to vector bosons as compared to that of a SM Higgs boson, and t_i , b_i are the corresponding ratios of the couplings to top and bottom quarks. (The coupling ratio for τ leptons is always the same as for b quarks, *i.e.* $\tau_i = b_i$). Note that we always have $|R_i| < 1$, but t_i and b_i can be larger, smaller or even differ in sign with respect to the SM. For the CP-odd Higgs bosons, there is no tree-level coupling to the VV states; t'_j and b'_j are defined as the ratio of the $i\gamma_5$ couplings for $t\bar{t}$ and $b\bar{b}$, respectively, relative to SM-like strength. We have also taken into account the contributions of the “difficult” decay modes $i) - viii)$ to the total decay width when kinematically allowed.

The expected statistical significances for the processes 1) $gg \rightarrow h/a \rightarrow \gamma\gamma$ and 6) $gg \rightarrow h \rightarrow WW^{(*)} \rightarrow \ell^+\ell^-\nu\bar{\nu}$ are computed from results for the SM Higgs boson taken from Ref. [8], Fig. 1. The application of the NMSSM corrections using R_i , t_i and b_i (which determine $\Gamma(gg \rightarrow h_i)$, $BR(h_i \rightarrow \gamma\gamma)$ and $BR(h_i \rightarrow WW^*)$) is straightforward in these two cases. The expected statistical significances for process 2) Wh/a or $t\bar{t}h/a$ with $\gamma\gamma\ell^\pm$ in the final state, are taken from the same figure. One finds that Wh_i and $t\bar{t}h_i$ production contribute with roughly equal weight to the SM signal. This allows us to decompose the expected significance into the corresponding production processes, apply the NMSSM corrections, and then recombine the production processes.

For the Standard Model Higgs boson, the expected statistical significances for process 3) $t\bar{t}h/a$ with $h/a \rightarrow b\bar{b}$, are taken from table 19-8 in Ref. [9], with the extension to Higgs boson masses above 120 GeV as provided by [15]. For the standard model process 5) $gg \rightarrow h \rightarrow ZZ^{(*)} \rightarrow 4$ leptons, we again use Ref. [9], tables 19-18 and 19-21. In both cases, the application of the NMSSM corrections is straightforward. The estimation of the statistical significances for the process 4) $b\bar{b}h/a$ with $h/a \rightarrow \tau^+\tau^-$, is more involved. Figure 19-62 of Ref. [9] give the 5σ contours in the $\tan\beta - m_A$ plane of the MSSM. The critical issue is how much of these 5σ signals derive from $gg \rightarrow H + gg \rightarrow A$ production and how much from associated $b\bar{b}H + b\bar{b}A$ production, and how each of the gg fusion and $b\bar{b}$ associated production processes are divided up between H and A . For more details on our procedure, see Ref. [5].

Results for the statistical significances of the h_i signals in modes 7) $WW \rightarrow h \rightarrow \tau^+\tau^-$ and 8) $WW \rightarrow h \rightarrow WW^{(*)}$ were similarly obtained by rescaling the theoretical results of [11].

In the case of Higgs states close in mass, the individual statistical significances have to be recombined. We used the procedure of Ref. [16], which gives the combined statistical significance $N_{SD,12}$ as a function of the individual statistical significances $N_{SD,1}$, $N_{SD,2}$ for two states with masses m_1, m_2 if $|m_1 - m_2| < \Delta_k \frac{m_1 + m_2}{2}$, where Δ_k is the mass resolution of the decay mode k):

$$N_{SD,12}^2 = N_{SD,1}^2 + N_{SD,2}^2 + 2 \frac{N_{SD,1} N_{SD,2}}{1 + (\frac{2}{\Delta_k} \frac{m_1 - m_2}{m_1 + m_2})^2}. \quad (7)$$

For the processes 1) – 8), we assumed $\Delta_{1,2,5,6} = 1\%$, $\Delta_{3,7,8} = 10\%$, and $\Delta_4 = 15\%$.

Using the above procedures, for each point in the parameter space of the NMSSM we obtain the statistical significances predicted for an integrated luminosity of 100 fb^{-1} for each of the detection modes 1) – 8). In order to obtain the statistical significances for the various detection modes at 300 fb^{-1} , we multiply the 100 fb^{-1} statistical significances by $\sqrt{3}$ in the cases 1), 2), 3), 5) and 6), but only by a factor of 1.3 in the cases 4), 7) and 8). That such a factor is appropriate for mode 4), see, for example, Fig. 19-62 in [9]. Use of this same factor for modes 7) and 8) is simply a conservative guess.

In our set of randomly scanned points defined in section 2, we selected those for which all the statistical significances [including WW -fusion modes 7) and 8)] are below 5σ . We obtained a lot of points, all with similar characteristics. Namely, in the Higgs spectrum, we always have a very SM-like CP-even Higgs boson with a mass between 115 and 135 GeV (*i.e.* above the LEP limit), which can be either h_1 or h_2 , with a reduced coupling to the gauge bosons $R_1 \simeq 1$ or $R_2 \simeq 1$, respectively. This state decays dominantly to a pair of (very) light CP-odd states, $a_1 a_1$, with m_{a_1} between 5 and 65 GeV¹. The singlet component of a_1 has to be small in order to have a large $h_1 \rightarrow a_1 a_1$ or $h_2 \rightarrow a_1 a_1$ branching ratio when the h_1 or h_2 , respectively, is the SM-like Higgs boson. Further, when the h_1 or h_2 is very SM-like, one has $R'_{11} \simeq 0$ or $R'_{21} \simeq 0$, respectively, so that the $e^+ e^- \rightarrow h_1 a_1$ or $e^+ e^- \rightarrow h_2 a_1$ associated production rate is very small and these processes thus place no constraint on the light CP-odd state at LEP. We have selected six difficult benchmark points. For points 1 – 3, h_1 is the SM-like CP-even state, while for points 4 – 6 it is h_2 . We have chosen the points so that $h_{1,2}$ and a_1 have different masses. The main characteristics of the benchmark points are displayed in table 1. Note the large branching ratios of the SM-like Higgs boson (h_1 for points 1 – 3 and h_2 for points 4 – 6) to decay to $a_1 a_1$. Branching ratios for the non-SM-like h_2 (points 1 – 3) or h_1 (points 4 – 6) are also shown. For points 4 – 6, with $m_{h_1} < 100 \text{ GeV}$, the h_1 is mainly singlet. As a result, R'_{11} is very small and thus there are no LEP constraints on the h_1 and a_1 from $e^+ e^- \rightarrow h_1 a_1$ production.

In the case of the points 1 – 3, the tabulated branching ratios of the h_2 are all very small. Even though the h_2 is heavy, it has very weak WW , ZZ coupling and $BR(h_2 \rightarrow ZZ + WW) \sim 0.01$. Further, the h_2 production rate due to gg fusion is greatly suppressed, as indicated in the table, as is its production rate from WW , ZZ fusion. This means that searches for the h_2 in the $ZZ \rightarrow 4\ell$ final state are impossible. In fact, the h_2 decays primarily to $t\bar{t}$ with the 2nd most important mode being Za_1 . The only search channel for the h_2 that might be worth further investigation appears to be the $b\bar{b}h_2$ Yukawa “radiation” process with $h_2 \rightarrow t\bar{t}$. Even though the $b\bar{b}h_2$ Yukawa couplings are somewhat enhanced, the overall production rate will not be that large and we anticipate that the signal for the h_2 in this mode would be quite marginal. Regarding the LC, since $m_{h_2} \gtrsim 500 \text{ GeV}$, $\sqrt{s_{e^+ e^-}}$ substantially above the 500 GeV level would be required. Even for such $\sqrt{s_{e^+ e^-}}$, h_2 detection would be very challenging since the ZZh_2 , WWh_2 couplings are very suppressed and the $b\bar{b}h_2$ Yukawa coupling is only somewhat enhanced. Thus, we have focused on the $a_1 a_1$ decays of the h_1 for points 1 – 3.

For points 4 – 6, even though the h_1 is quite light, it is dominantly singlet-like and therefore has suppressed couplings to all relevant SM particles, WW , ZZ , $b\bar{b}$ and $t\bar{t}$. As a result, it has very low production rates and its decays (primarily to either $b\bar{b}$, points

¹In some rare cases, one has h_2 decaying mainly to $h_1 h_1$, but then the LHC significances corresponding to the discovery channels 1) — 8) are quite close to 5, so we have not considered cases of this type.

Point Number	1	2	3	4	5	6
Bare Parameters						
λ	0.2872	0.2124	0.3373	0.3340	0.4744	0.5212
κ	0.5332	0.5647	0.5204	0.0574	0.0844	0.0010
$\tan \beta$	2.5	3.5	5.5	2.5	2.5	2.5
μ_{eff} (GeV)	200	200	200	200	200	200
A_λ (GeV)	100	0	50	500	500	500
A_κ (GeV)	0	0	0	0	0	0
CP-even Higgs Boson Masses and Couplings						
m_{h_1} (GeV)	115	119	123	76	85	51
R_1	1.00	1.00	-1.00	0.08	0.10	-0.25
t_1	0.99	1.00	-1.00	0.05	0.06	-0.29
b_1	1.06	1.05	-1.03	0.27	0.37	0.01
Relative gg Production Rate	0.97	0.99	0.99	0.00	0.01	0.08
$BR(h_1 \rightarrow b\bar{b})$	0.02	0.01	0.01	0.91	0.91	0.00
$BR(h_1 \rightarrow \tau^+\tau^-)$	0.00	0.00	0.00	0.08	0.08	0.00
$BR(h_1 \rightarrow a_1 a_1)$	0.98	0.99	0.98	0.00	0.00	1.00
m_{h_2} (GeV)	516	626	594	118	124	130
R_2	-0.03	-0.01	0.01	-1.00	-0.99	-0.97
t_2	-0.43	-0.30	-0.10	-0.99	-0.99	-0.95
b_2	2.46	-3.48	3.44	-1.03	-1.00	-1.07
Relative gg Production Rate	0.18	0.09	0.01	0.98	0.99	0.90
$BR(h_2 \rightarrow b\bar{b})$	0.01	0.04	0.04	0.02	0.01	0.00
$BR(h_2 \rightarrow \tau^+\tau^-)$	0.00	0.01	0.00	0.00	0.00	0.00
$BR(h_2 \rightarrow a_1 a_1)$	0.04	0.02	0.83	0.97	0.98	0.96
m_{h_3} (GeV)	745	1064	653	553	554	535
CP-odd Higgs Boson Masses and Couplings						
m_{a_1} (GeV)	56	7	35	41	59	7
t'_1	0.05	0.03	0.01	-0.03	-0.05	-0.06
b'_1	0.29	0.34	0.44	-0.20	-0.29	-0.39
Relative gg Production Rate	0.01	0.03	0.05	0.01	0.01	0.05
$BR(a_1 \rightarrow b\bar{b})$	0.92	0.00	0.93	0.92	0.92	0.00
$BR(a_1 \rightarrow \tau^+\tau^-)$	0.08	0.94	0.07	0.07	0.08	0.90
m_{a_2} (GeV)	528	639	643	560	563	547
Charged Higgs Mass (GeV)	528	640	643	561	559	539
Most Visible Process No.	2 (h_1)	2 (h_1)	8 (h_1)	2 (h_2)	8 (h_2)	8 (h_2)
Significance at 300 fb^{-1}	0.48	0.26	0.55	0.62	0.53	0.16

Table 1: Properties of selected scenarios that could escape detection at the LHC. In the table, R_i , t_i and b_i are the ratios of the h_i couplings to VV , $t\bar{t}$ and $b\bar{b}$, respectively, as compared to those of a SM Higgs boson with the same mass; t'_1 and b'_1 denote the magnitude of the $i\gamma_5$ couplings of a_1 to $t\bar{t}$ and $b\bar{b}$ normalized relative to the magnitude of the $t\bar{t}$ and $b\bar{b}$ SM Higgs couplings. We also give the production for $gg \rightarrow h_i$ fusion relative to the gg fusion rate for a SM Higgs boson with the same mass. Important absolute branching ratios are displayed. For points 2 and 6, $BR(a_1 \rightarrow jj) \simeq 1 - BR(a_1 \rightarrow \tau^+\tau^-)$. For the heavy h_3 and a_2 , we give only their masses. In the case of the points 2 and 6, decays of a_1 into light quarks start to contribute. For all points 1 – 6, the statistical significances for the detection of any Higgs boson in any of the channels 1) – 8) (as listed in the introduction) are tiny; their maximum is indicated in the last row, together with the process number and the corresponding Higgs state.

4 and 5, or $a_1 a_1$, point 6) will not produce particularly distinctive final states, especially given the smallness of m_{h_1} . Thus, we believe the h_1 would be very difficult to detect at the LHC. At the LC, the h_1 has ZZ coupling sufficient for detection only in the case of point 6. Given the complicated nature of the $h_1 \rightarrow a_1 a_1$ final state in this case (including the fact that the a_1 is so light that $a_1 \rightarrow \tau^+ \tau^-$ is dominant) detection would have to rely on the ZX reconstructed recoil mass technique. Thus, for points 4 – 6, we will focus on searching for the SM-like h_2 in its dominant $h_2 \rightarrow a_1 a_1$ decay mode.

Of course, we should also consider whether or not the h_3 or a_2 might be detectable for points 1 – 6. Since m_{h_3} is very large in all cases, one would need to rely on the $h_3 \rightarrow ZZ \rightarrow 4\ell$ mode [mode 5] in our first list] for its detection. But, the gg and WW fusion production rates are suppressed and $BR(h_3 \rightarrow ZZ) < 0.01$. Mode 5) for the h_3 contributes negligibly to the net statistical significance in the last column of table 1. At the LC, $\sqrt{s_{e^+ e^-}}$ substantially above 500 GeV would be required at all points. Detection of the a_2 would appear to be even more difficult. If a super high energy LC is eventually built, the pair production modes such as $e^+ e^- \rightarrow Z \rightarrow h_3 a_2$ will be substantial and produce very viable signals.

In the case of points 2 and 6, it should be noted that the $a_1 \rightarrow \tau^+ \tau^-$ decays are dominant, with $a_1 \rightarrow jj$ decays making up most of the rest. For points 1 and 3 – 5 for which $BR(a_1 \rightarrow b\bar{b})$ is substantial, the b jets will not be that energetic and tagging will be somewhat inefficient. Thus, we have chosen not to implement b -tagging as part of the experimental procedures detailed in the next section.

Finally, we should consider whether or not a direct search for the a_1 might be feasible. For our points 1 – 6, the a_1 has suppressed couplings to both $b\bar{b}$ and $t\bar{t}$ and will thus be very weakly produced via Yukawa radiation and would not be detectable in this way at either the LHC or the LC [17]. The only processes that would have significant rate are those relying on the $ZZ a_1 a_1$ and $WW a_1 a_1$ quartic couplings required by gauge invariance. At the LHC, the rate for, say, $WW \rightarrow a_1 a_1$ is not exactly large and, as we shall see, there is a large background from $t\bar{t}$ production. Rates for continuum $WW \rightarrow a_1 a_1$ production at the LC are substantial for a light a_1 [18], but again we shall see that there is a large background. In the next section, we demonstrate that the constraint that $M_{a_1 a_1} \sim m_h$ with $m_h \sim 100$ GeV is absolutely critical in order to have any hope of extracting a signal in $WW \rightarrow h$ production at both the LHC and the LC.

4 New Channels at the LHC and LC

As we have already stressed, for the points summarized in table 1 the a_1 is light and decays almost entirely into $b\bar{b}$ (or jj for points 2 and 6) and $\tau^+ \tau^-$. The possible final states are thus $b\bar{b}b\bar{b}$ (or $4j$ for points 2 and 6), $b\bar{b}\tau^+ \tau^-$ (or $2j\tau^+ \tau^-$) and $\tau^+ \tau^- \tau^+ \tau^-$. A 4 b -signal would be burdened by a large QCD background even after implementing b -tagging. A 4 j -signal would be completely swamped by QCD background. Meanwhile, the 4 τ -channel would not allow one to reconstruct the h_1, h_2 resonances. Hence, in attempting to cover these problematic points of the NMSSM parameter space at the LHC, we will focus in this study on the $2b2\tau$ (or $2j2\tau$) signature. The extra factor of two in $BR(a_1 a_1 \rightarrow b\bar{b}\tau^+ \tau^-) = 2BR(a_1 \rightarrow b\bar{b})BR(a_1 \rightarrow \tau^+ \tau^-)$ relative to $BR(a_1 a_1 \rightarrow b\bar{b}b\bar{b}) = [BR(a_1 \rightarrow b\bar{b})]^2$ and $BR(a_1 a_1 \rightarrow \tau^+ \tau^- \tau^+ \tau^-) = [BR(a_1 \rightarrow \tau^+ \tau^-)]^2$ (and similarly with $b\bar{b} \rightarrow jj$ for points 2 and 6) is an additional advantage. It compensates in part (or further increases) the

Yukawa suppression (or enhancement) with respect to the $h_1/h_2 \rightarrow a_1 a_1 \rightarrow 4b(4\tau)$ decay rate.² In addition, we will be looking at τ 's decaying leptonically to electrons and muons, yielding some amount of missing (transverse) momentum, p_{miss}^T , that could be projected onto the visible e, μ -momenta in an attempt to reconstruct the parent τ -direction. Since for points 2 and 6 the a_1 does not decay to $b\bar{b}$ and since the b and \bar{b} that do come from a_1 are not very energetic given the modest m_{a_1} mass for points 1 and 3 – 5, we will not employ b -tagging as part of our analysis.

4.1 Results for the LHC

Detection of WW^* and $\tau^+\tau^-$ decays of a relatively light Higgs boson with SM-like WW coupling is straightforward at the LHC in the vector-vector fusion production mode [*i.e.* the Higgs production channel entering the signatures 8) and 9)] when the light Higgs boson has mass above the LEP limits and decays directly to $\tau^+\tau^-$ (the status of the $b\bar{b}$ mode has not yet been determined). Because the significance of this type of signal for a SM-like Higgs boson is very large, we consider here the same WW -fusion production mode in the context of the NMSSM. (We reemphasize that the h_1 [cases 1 – 3] or h_2 [cases 4 – 6] has nearly full SM strength coupling to WW .) However, the $b\bar{b}\tau^+\tau^-$ (or $2j\tau^+\tau^-$, for points 2 and 6) final state of relevance is more complex and subject to larger backgrounds than is a simple $\tau^+\tau^-$ final state. Further, the a_1 masses of interest are only half as large as the Higgs masses for which the direct $h \rightarrow \tau^+\tau^-$ signals are viable. In order to extract the $2j2\tau$ NMSSM Higgs boson signature from the central detector region, we have exploited forward and backward jet tagging on the light quarks emerging after the double W -strahlung preceding WW -fusion, the utility of which is reviewed in Ref. [19]. If we require two additional forward/backward jets, it is clear that the leading background is due to $t\bar{t}$ production (since we are assuming a heavy SUSY spectrum) and decay via the purely SM process,

$$gg \rightarrow t\bar{t} \rightarrow b\bar{b}W^+W^- \rightarrow b\bar{b}\tau^+\tau^- + p_{\text{miss}}^T, \quad (8)$$

in association with forward and backward jet radiation.

In summary, at the LHC, the signature is

- 2 forward/backward jets, at least 2 central jets, p_{miss}^T and a $\tau^+\tau^-$ pair decaying leptonically (to electrons and/or muons).

In order to carry out realistic numerical simulations, we have used a modification of the MSSM implementation [20] of the **HERWIG** event generator [21], in conjunction with the **GETJET** code [22] for calorimeter emulation and jet reconstruction. An **ISAWIG** format [23] input file has been edited by hand to incorporate the Higgs boson mass spectrum and decay rates as predicted for each of the NMSSM points 1 – 6, while in the main **HERWIG** code (v6.4) the subroutine implementing the vector-vector fusion process has been modified to account for the different Higgs- VV vertices pertaining to the NMSSM points 1 – 6 given in table 1. The above codes do not include K factors for either the signal or the background.

An outline of the selection procedure and cuts used is the following.

²Recall that it is the running b -quark mass (evaluated at the a_1 mass) that enters the Yukawa coupling, rather than the pole mass.

- Acceptance cuts:

$$|\eta_{\text{jet}}| < 5, \quad p_{\text{jet}}^T > 20 \text{ GeV}, \quad \Delta R_{\text{jet-jet}} > 0.7,$$

$$\eta_{\text{jet}}^{\max} \cdot \eta_{\text{jet}}^{\min} < 0, \quad |\eta_{\text{lepton}}| < 2.5,$$

$$p_{\text{lepton}}^T > 10 \text{ GeV}, \quad \text{no lepton isolation.}$$

- Since the a_1 will not have been detected previously, we must assume a value for m_{a_1} . It will be necessary to repeat the analysis for densely spaced m_{a_1} values and look for the m_{a_1} choice that produces the best signal.
- We look among the central jets for the combination with invariant mass M_{jj} closest to m_{a_1} (no b -tagging is enforced, b 's are identified as non-forward/backward jets).
- Select the two highest transverse-momentum leptons in any flavor combination and with opposite charge. After ensuring that these are not back-to-back (by requiring that their relative angle is smaller than 175 degrees), resolve the p_{miss}^T along their directions and reconstruct the invariant mass, $M_{\tau^+\tau^-}$.
- Plot the $M_{jj\tau^+\tau^-}$ invariant mass using the four four-momenta reconstructed in the two previous steps, as seen in the top plot of Fig. 1 — the plot presented assumes that we have hit on the correct m_{a_1} choice.

The selection strategy adopted is clearly efficient in reconstructing the h_1 (for points 1–3) and h_2 (for points 4–6) masses from the $jj\tau^+\tau^-$ system, as one can appreciate by noting the peaks appearing in the LHC plot of Fig. 1 at $M_{jj\tau^+\tau^-} \approx 100$ GeV. In contrast, the heavy Higgs resonances at m_{h_2} for points 1–3 and the rather light resonances at m_{h_1} for points 4–6 (recall table 1) do not appear, the former mainly because of the very poor production rates and the latter due to the fact that either the $h_1 \rightarrow a_1 a_1$ decay mode is not open (points 4, 5) or – if it is – the b -quarks and e/μ -leptons eventually emerging from the a_1 decays are too soft to pass the acceptance cuts (point 6, for which $m_{a_1} = 7$ GeV and $m_{h_1} = 51$ GeV). For all six NMSSM setups, one may see a hint of a resonance in the data in the very end of the low mass tail of the $t\bar{t}$ background (see the insert in the top frame of Fig. 1). However, after summing the background distribution and any one of the signal spectra, it could be difficult to ascertain the existence of the h_1 or h_2 peaks from the net line shapes. Still, statistics are significant. To estimate S/\sqrt{B} , we assume $L = 300 \text{ fb}^{-1}$, a K factor of 1.1 for WW fusion and a K factor of 1.6 for the $t\bar{t}$ background. (These K factors are not included in the plots of Fig. 1.) We sum events over the region $60 \leq M_{jj\tau^+\tau^-} \leq 90$ GeV. For points 1–6 we obtain signal rates of about $S = 890, 600, 750, 1030, 915, 500$, respectively. The $t\bar{t}$ background rate is $B \sim 320$. This gives $N_{SD} = S/\sqrt{B}$ of 50, 34, 42, 58, 51, 28 for points 1–6, respectively. These are substantial. However, given the broad distribution of the signal, it is clear that the crucial question will be the accuracy with which the background shape can be predicted from theory. The background *normalization* after the cuts imposed in our analysis would be very well known from the higher $M_{jj\tau^+\tau^-}$ regions.

4.2 The LC scenario

While further examination of and refinements in the LHC analysis may ultimately lead us to have full confidence in the viability of the NMSSM Higgs boson signals discussed

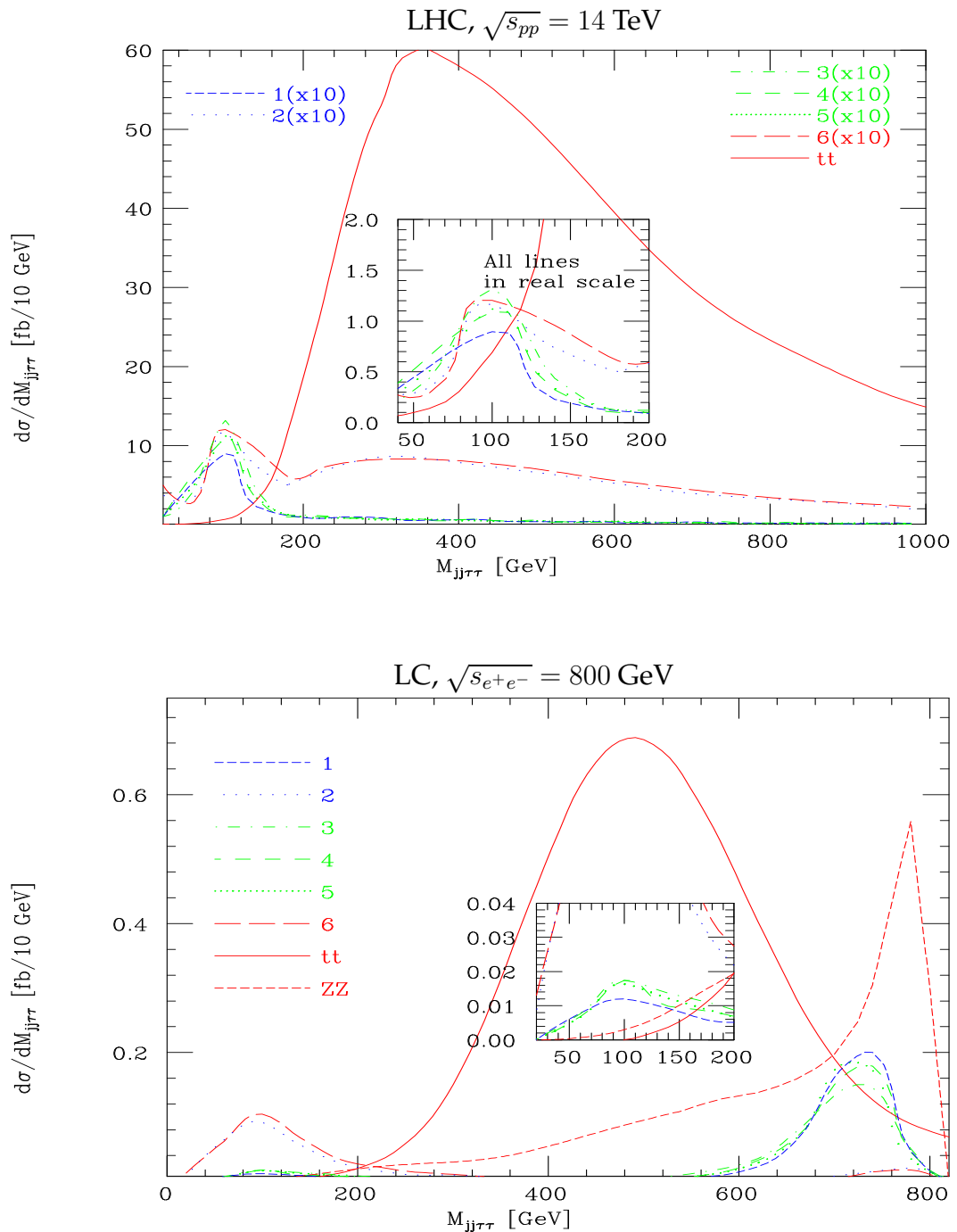


Figure 1: Reconstructed mass of the $jj\tau^+\tau^-$ system for signals and backgrounds after the selections described, at the LHC (top) and a LC (bottom). We plot $d\sigma/dM_{jj\tau^+\tau^-}$ [fb/10 GeV] vs $M_{jj\tau^+\tau^-}$ [GeV] using GETJET and HERWIG 6.4 with: $\text{IPROC}=3720$ adapted to NMSSM couplings and decay rates for the signal and $\text{IPROC}=1706$ for the background at the LHC; $\text{IPROC}=920$ adapted to NMSSM couplings and decay rates for the signal and $\text{IPROC}=126$ (250) for the $t\bar{t}[ZZ]$ background at a LC). Statistics used: 500,000 points. Normalization is to the total cross section after cuts. In both plots, the lines corresponding to points 4 and 5 are visually indistinguishable. No K factors are included.

above, an enhancement at low $M_{jj\tau^+\tau^-}$ of the type shown (for some choice of m_{a_1}) will nonetheless be the only evidence on which a claim of LHC observation of Higgs bosons can be based. Ultimately, a means of confirmation and further study will be critical. Thus, it is important to summarize the prospects at the LC, with energy up to 800 GeV, for detecting the NMSSM Higgs bosons, especially in the context of the difficult scenarios 1—6 of table 1 discussed here. As we summarize below, the LC is certainly guaranteed to find the h_1 (points 1–3) or the h_2 (points 4–6) and will allow a good determination of the $h_1 a_1 a_1$ or $h_2 a_1 a_1$ branching ratio, respectively, a possibly very important piece of information for unraveling the model. In these scenarios, the LC would be an absolutely essential complement to the LHC, and, in particular, would be the only machine at which precision Higgs physics studies could be pursued. In what follows, we will use the notation h for $h = h_1$ for points 1–3 and $h = h_2$ for points 4–6 in table 1.

Because the ZZh coupling is nearly full strength in all cases, and because the h mass is of order 100 GeV, discovery of the h will be very straightforward via $e^+e^- \rightarrow Zh$ using the $e^+e^- \rightarrow ZX$ reconstructed M_X technique which is independent of the “unexpected” complexity of the h decay to $a_1 a_1$. This will immediately provide a direct measurement of the ZZh coupling with very small error [24]. The next stage will be to look at rates for the various h decay final states, F , and extract $BR(h \rightarrow F) = \sigma(e^+e^- \rightarrow Zh \rightarrow ZF)/\sigma(e^+e^- \rightarrow Zh)$. For the NMSSM points considered here, the main channels would be $F = b\bar{b}b\bar{b}$, $F = b\bar{b}\tau^+\tau^-$ and $F = \tau^+\tau^-\tau^+\tau^-$.³ At the LC, a fairly accurate determination of $BR(h \rightarrow F)$ should be possible in all three cases. This is important if we are to be able to determine $BR(h \rightarrow a_1 a_1)$ independently. The procedure is the following. From

$$\begin{aligned} BR(h \rightarrow b\bar{b}b\bar{b}) &= BR(h \rightarrow a_1 a_1) [BR(a_1 \rightarrow b\bar{b})]^2 \\ BR(h \rightarrow \tau^+\tau^-\tau^+\tau^-) &= BR(h \rightarrow a_1 a_1) [BR(a_1 \rightarrow \tau^+\tau^-)]^2 \\ BR(h \rightarrow b\bar{b}\tau^+\tau^-) &= 2BR(h \rightarrow a_1 a_1) BR(a_1 \rightarrow b\bar{b}) BR(a_1 \rightarrow \tau^+\tau^-), \end{aligned} \quad (9)$$

we see that $BR(a_1 \rightarrow \tau^+\tau^-)/BR(a_1 \rightarrow b\bar{b})$ can be determined using two independent ratios. Assuming that these are the only two decay channels (as can be checked by looking for other final states), the requirement $BR(a_1 \rightarrow \tau^+\tau^-) + BR(a_1 \rightarrow b\bar{b}) = 1$ then allows extraction of the individual BR ’s. Once these are known, we can use the above equations to determine $BR(h \rightarrow a_1 a_1)$. Certainly, this procedure will be carried out in the $e^+e^- \rightarrow Zh$ production mode. However, we have not performed the required simulation for this paper to determine the actual accuracy that can be achieved.

Instead, we have considered the equally (or perhaps more) useful vector-vector fusion mode that will be active at a LC. In fact, at 800 GeV or above, it is the dominant Higgs boson production channel for CP-even Higgs bosons in the intermediate mass range. Contrary to the case of the LHC though, the dominant contribution (from WW fusion) does not allow for forward and backward particle tagging, as the incoming electron and positron convert into (anti)neutrinos, which escape detection. Although the ZZ fusion contribution would allow tagging of forward/backward e^- and e^+ , the cross section is a factor of 10 smaller (see Fig. 4 of Ref. [24]) in comparison. Still, since the $t\bar{t}$ background would not typically be accompanied by forward/backward e^+ and e^- in e^+e^- collisions, unless initiated by $\gamma\gamma$ interactions (which tend to produce less energetic $t\bar{t}$ pairs), tagging of the electron and positron in the final state might offer a handle against the $t\bar{t}$ noise.

³Here, and in the following discussion, $b\bar{b}$ should be replaced by jj for points 2 and 6, where j refers to any possible non- b jet.

But, in any case it seems unnecessary to focus on ZZ fusion given that $t\bar{t}$ production at the LC proceeds through EW interactions, rather than via QCD as at the LHC. Indeed, in going from the LHC to a LC, the $t\bar{t}$ production rate should be reduced (apart from parton distribution functions) by a factor of $\mathcal{O}(\alpha_s/\alpha_{\text{em}})^2$ with respect to the vector boson fusion Higgs boson signal (which is an electroweak process at both the LC and the LHC). A new background of importance does emerge at the LC, namely ZZ -pair production with one Z decaying to jj and the other to $\tau^+\tau^-$ pairs. The ZZ background is negligible at the LHC mainly because associated energetic forward/backward jets from QCD initial state radiation are infrequent. At the LC, the ZZ background plays a more significant role and has been simulated in our `HERWIG` and (LC-adjusted) `GETJET` numerical analysis.

At a LC, the optimal signature will thus be different than at the LHC and a different set of selection criteria are needed. We choose selection criteria that will retain both the WW and the ZZ fusion Higgs boson production processes.

- We require an even number of oppositely-charged leptons ($n_\ell = 2, 4\dots$).
- If $n_\ell \geq 4$ then we demand that two of these must be an electron and a positron, so that the final state would be consistent with having been generated by forward/backward e^\pm tagging in ZZ -fusion and $\tau^+\tau^-$ decays in which both τ 's decay leptonically (to electron and muons).
- Finally, we require at least 2 central jets and significant p_{miss}^T .

Given the required final state as above, we employ the following selection procedure and cuts.

- Acceptance cuts:

$$\begin{aligned} |\cos \theta_{\text{jet}}| &< 0.990, & p_{\text{jet}}^T &> 5 \text{ GeV}, & \Delta R_{\text{jet-jet}} &> 0.4, \\ \eta_{e^+}^{\text{max}} \cdot \eta_{e^-}^{\text{min}} &< 0 \text{ (if } n_\ell \geq 4\text{)}, & |\cos \theta_{\text{lepton}}| &< 0.995, \\ p_{\text{lepton}}^T &> 5 \text{ GeV}, & \text{no lepton isolation.} \end{aligned}$$

- We look among the central jets for the combination with invariant mass M_{jj} closest to m_{a_1} (again, no b -tagging is enforced — b 's are identified as non-forward/backward jets).
- Out of the n_ℓ leptons, upon excluding the e^+e^- pair in which the electron and positron are those with the largest rapidities if $n_\ell \geq 4$, select the two with highest transverse-momenta in any flavor combination and with opposite charge.

After ensuring that these are not back-to-back, resolve the p_{miss}^T along their directions and reconstruct the invariant mass $M_{\tau^+\tau^-}$.

- Plot the $M_{jj\tau^+\tau^-}$ invariant mass (see the bottom of Fig. 1) using the four four-momenta reconstructed in the two previous steps.

Note that it is not fruitful to place cuts on the invariant masses M_{jj} and $M_{\tau^+\tau^-}$ that exclude $M_{jj}, M_{\tau^+\tau^-} \sim m_Z$ in an attempt to reduce the ZZ background. This is because the SM-like h mass is typically of order 115 GeV, *i.e.* not so far from m_Z , and the experimental resolutions in the two masses M_{jj} and $M_{\tau^+\tau^-}$ are poor, either because of the large

number of hadronic tracks or the missing longitudinal momenta of the (anti) neutrinos, respectively.

Just as at the LHC, the peaks corresponding to the Higgs boson with weak VV coupling (h_2 for points 1 – 3 and h_1 for points 4 – 6) do not appear in the $M_{jj\tau^+\tau^-}$ distribution which can be reconstructed at a LC. Here, though, for the visible h (h_1 for points 1 – 3, h_2 for points 4 – 6) the situation is better than at the LHC. For all points 1 – 6 the mass peaks (again centered at 100 GeV) are now very clearly visible above both the $t\bar{t}$ and ZZ backgrounds, particularly for the case of points 2 and 6 (see insert in the bottom frame of Fig. 1). Assuming $L = 500 \text{ fb}^{-1}$, the points 1,3,4,5 yield 5 events per 10 GeV bin, on average, in the 50 to 150 GeV mass interval of interest. This would constitute a convincing signal given the very small size predicted for the background. Notice that, although to assign the entire missing transverse momentum to the τ -lepton system may seem not entirely appropriate (as it is largely due to forward/backward (anti)neutrinos from the incoming electrons and positrons in WW fusion), this does not hamper the ability to reconstruct the Higgs mass peaks. However, this implies that a proportion of the signal events will tend to reproduce the overall $\sqrt{s_{e^+e^-}}$ value in the $M_{jj\tau^+\tau^-}$ distribution. The effect is more pronounced for points 1 and 3–5, which is where the a_1 mass is larger (see Table 1) so that most of the hadronic tracks composing the emerging jets easily enter the detector region. For points 2 and 6, where m_{a_1} is below 10 GeV, this may often not be true and it appears that the consequent effect of these hadrons escaping detection is that of counterbalancing the p_{miss}^T contributions related to the neutrinos left behind in WW fusion reactions. For the case of the ZZ noise, in the presence of full coverage and perfect resolution of the detector, one would have $M_{jj\tau^+\tau^-} \equiv \sqrt{s_{e^+e^-}}$, which explains the very noticeable preference for this process to produce a concentration of events with $M_{jj\tau^+\tau^-}$ around 800 GeV in the mass distribution. (The “tails” beyond $\sqrt{s_{e^+e^-}}$ are due to the smearing of the visible tracks in our Monte Carlo analysis.)

Finally notice that we have included Initial State Radiation (ISR) and beam-strahlung effects, as predicted using the `HERWIG` default. These tend to introduce an additional unresolvable missing longitudinal momentum, although to a much smaller extent than do the Parton Distribution Functions (PDFs) in hadron-hadron scattering at the LHC.

A final note regarding WW, ZZ fusion to h . Since we will know from Zh production the magnitude of the WWh and ZZh coupling, the rate for $e^+e^- \rightarrow ZZ, WW \rightarrow h \rightarrow b\bar{b}\tau^+\tau^-$ will determine $BR(h \rightarrow b\bar{b}\tau^+\tau^-)$, with similar results perhaps possible for other channels. Thus, we could hope to implement the procedure described earlier for extracting $BR(h \rightarrow a_1a_1)$ using both $WW, ZZ \rightarrow h$ fusion and Zh production.

5 Conclusions

In summary, if the NMSSM parameters are such that the most SM-like of the CP-even Higgs bosons, h , is relatively light and decays primarily to a pair of CP-odd Higgs states, $h \rightarrow aa$, then there will be a statistically highly significant LHC signal (from $WW \rightarrow h \rightarrow aa$) of an $S/B \sim (500 - 1000)/300$ bump (for $L = 300 \text{ fb}^{-1}$) in the low-mass tail of a rapidly falling $jj\tau^+\tau^-$ mass distribution. The LHC would thus give a very strong indication of the presence of a Higgs boson. However, this detection mode is not exactly in the gold-plated category. The LC will be absolutely essential in order to confirm that the enhancement seen at the LHC really does correspond to a Higgs boson. At the LC, discovery of a light

SM-like h is guaranteed to be possible in the Zh final state using the recoil mass technique. Further, we have seen that WW, ZZ fusion production of the h will also produce a viable signal in the $jj\tau^+\tau^-$ final state (and perhaps in the $4j$ and $\tau^+\tau^-\tau^+\tau^-$ final states as well, although we have not examined these [25]).⁴ Measurement of the relative rates for the $4j, 2j2\tau$ and 4τ final states will allow a determination of the $a \rightarrow jj$ and $a \rightarrow \tau^+\tau^-$ branching ratios, which in turn will make possible the determination of $BR(h \rightarrow aa)$, a potentially very important measurement. Unfortunately, the standard techniques for determining the total width of a SM-like h relying on the $\gamma\gamma$ and/or WW final state decays of the h will not be available and it is thus unlikely that we can convert a measurement of $BR(h \rightarrow aa)$ into a determination of the partial width $\Gamma(h \rightarrow aa)$ (which would be most directly related to the very interesting haa coupling strength). As we have stressed, for parameter space points of the type we have discussed here, detection of any of the other MSSM Higgs bosons is likely to be impossible at the LHC and is likely to require an LC with $\sqrt{s_{e^+e^-}}$ above the relevant thresholds for $h'a'$ production, where h' and a' are heavy CP-even and CP-odd Higgs bosons, respectively. Although results for the LHC indicate that Higgs boson discovery will be challenging for the type of situations we have considered, improved techniques for extracting a signal are likely to be developed once data is in hand and the $t\bar{t}$ background can be more completely modeled. Clearly, if SUSY is discovered and no Higgs bosons are detected in the standard MSSM modes, a careful search for the signal we have considered should have a high priority. Finally, we should remark that the $h \rightarrow aa$ search channel considered here in the NMSSM framework is also highly relevant for a general two-Higgs-doublet model, 2HDM. It is really quite possible that the most SM-like CP-even Higgs boson of a 2HDM will decay primarily to two CP-odd states. This is possible even if the CP-even state is quite heavy, unlike the NMSSM cases considered here.

Acknowledgments

JFG is supported by the U.S. Department of Energy and the Davis Institute for High Energy Physics. SM thanks the UK-PPARC for financial support and D.J. Miller for useful conversations. CH is supported by the European Commission RTN grant HPRN-CT-2000-00148. JFG, CH, and UE thank the France-Berkeley fund for partial support of this research.

References

- [1] J. R. Ellis, J. F. Gunion, H. E. Haber, L. Roszkowski and F. Zwirner, Phys. Rev. D **39** (1989) 844.
- [2] H.P. Nilles, M. Srednicki and D. Wyler, Phys. Lett. **120 B** (1983) 346; M. Drees, Int. J. Mod. Phys. **A 4** (1989) 3635; U. Ellwanger and M. Rausch de Traubenberg, Z. Phys. **C 53** (1992) 521; P.N. Pandita, Z. Phys. **C 59** (1993) 575; Phys. Lett. **B 318** (1993) 338; T. Elliot, S.F. King and P.L. White, Phys. Rev. **D 49** (1994) 2435;

⁴For many, but not all, parameter choices of interest, $jj = b\bar{b}$.

U. Ellwanger and C. Hugonie, Eur. Phys. J. **C 5** (1998) 723;
 A. Dedes, C. Hugonie, S. Moretti and K. Tamvakis, Phys. Rev. **D 63** (2001) 055009.

[3] J.-P. Derendinger, C.A. Savoy, *Nucl. Phys.* **B 237** (1984) 307;
 M. Drees, *Int. J. Mod. Phys.* **A 4** (1989) 3635;
 J. R. Espinosa, M. Quiros, *Phys. Lett. B* **279** (1992) 92;
 P. Binetruy, C.A. Savoy, *Phys. Lett. B* **277** (1992) 453.

[4] U. Ellwanger, M. Rausch de Traubenberg, C.A. Savoy, *Phys. Lett. B* **315** (1993) 331, *Z. Phys. C* **67** (1995) 665, *Nucl. Phys. B* **492** (1997) 21;
 J. Kamoshita, Y. Okada, M. Tanaka, *Phys. Lett. B* **328** (1994) 67;
 F. Franke, H. Fraas, *Phys. Lett. B* **353** (1995) 234;
 S.F. King, P.L. White, *Phys. Rev. D* **52** (1995) 4183 and *Phys. Rev. D* **53** (1996) 4049;
 S. Ham, S. Oh, B. Kim, *Phys. Lett. B* **414** (1997) 305;
 N. Krasnikov, *Mod. Phys. Lett. A* **13** (1998) 893;
 D. J. Miller, R. Nevzorov and P. M. Zerwas, arXiv:hep-ph/0304049.

[5] U. Ellwanger, J. F. Gunion and C. Hugonie, arXiv:hep-ph/0111179.

[6] LEP Higgs Working Group, Note 2002/01.

[7] LEP Higgs Working Group, Note 2001/04.

[8] CMS Collaboration, “Expected Observability of Standard Model Higgs in CMS with 100 fb^{-1} ”, CMS NOTE 1997/057.

[9] ATLAS Collaboration, “Detector and Physics Performance Technical Design Report Vol. II (1999)”, CERN/LHCC/99-15 p. 675–811.

[10] D. Zeppenfeld, R. Kinnunen, A. Nikitenko and E. Richter-Was, *Phys. Rev. D* **62** (2000) 013009.

[11] D. Zeppenfeld, in *Proc. of the APS/DPF/DPB Summer Study on the Future of Particle Physics (Snowmass 2001)* ed. N. Graf, eConf **C010630**, P123 (2001).

[12] U. Ellwanger and C. Hugonie, Eur. Phys. J. **C 25** (2002) 297.

[13] A. Djouadi, M. Spira and P. M. Zerwas, *Z. Phys. C* **70** (1996) 427.

[14] A. Djouadi, J. Kalinowski and M. Spira, *Comput. Phys. Commun.* **108** (1998) 56.

[15] We thank M. Sapinski for providing us with this extension, based on the same techniques as employed in the ATLAS analysis, as part of the Les Houches 2001 workshop.

[16] E. Richter-Was, D. Froidevaux, F. Gianotti, L. Poggioli, D. Cavalli and S. Resconi, *Int. J. Mod. Phys. A* **13** (1998) 1371.

[17] B. Grzadkowski, J. F. Gunion and J. Kalinowski, *Phys. Lett. B* **480**, 287 (2000).

[18] See T. Farris, J. F. Gunion and H. E. Logan, in *Proc. of the APS/DPF/DPB Summer Study on the Future of Particle Physics (Snowmass 2001)* ed. N. Graf, eConf **C010630**, P121 (2001) [arXiv:hep-ph/0202087], and references therein.

- [19] D. Cavalli *et al.*, arXiv:hep-ph/0203056.
- [20] S. Moretti, K. Odagiri, P. Richardson, M.H. Seymour and B.R. Webber, JHEP **04** (2002) 028; S. Moretti, preprint CERN-TH/2002-075, IPPP/02/22, DCPT/02/44, May 2002, arXiv:hep-ph/0205105.
- [21] G. Marchesini, B.R. Webber, G. Abbiendi, I.G. Knowles, M.H. Seymour and L. Stanco, Comput. Phys. Commun. **67** (1992) 465; G. Corcella, I.G. Knowles, G. Marchesini, S. Moretti, K. Odagiri, P. Richardson, M.H. Seymour and B.R. Webber, arXiv:hep-ph/9912396; JHEP **01** (2001) 010; arXiv:hep-ph/0107071; arXiv:hep-ph/0201201, arXiv:hep-ph/0210213.
- [22] S. Moretti, private program.
- [23] See <http://www-thphys.physics.ox.ac.uk/users/PeterRichardson/HERWIG/isawig.>
- [24] See, for example, the summary of J. F. Gunion, H. E. Haber and R. Van Kooten, "Higgs physics at the linear collider," arXiv:hep-ph/0301023.
- [25] U. Ellwanger, J.F. Gunion, C. Hugonie and S. Moretti, in progress.